Finite-Difference Time-Domain (FDTD) Voxels-In-Cell (VIC) Method

Kenan Tekbaş and Jean-Pierre Bérenger

Are Conformal Methods Really Conformal?

Yu, W., and R. Mittra, "A conformal finite difference time domain technique for modeling curved dielectric surfaces," IEEE Microwave Components Lett,, Vol. 11, 2001, pp. 25-27.

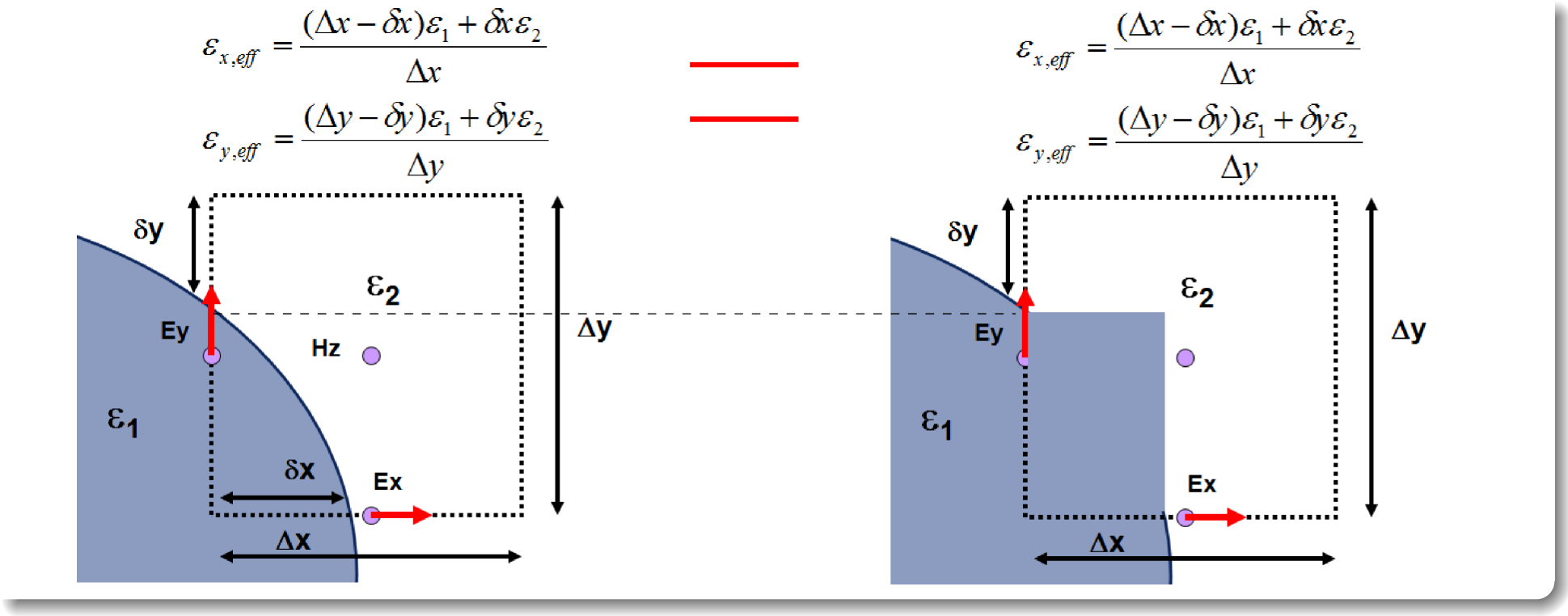

Ansys Lumerical: https://optics.ansys.com/hc/en-us/articles/360034382614-Selecting-the-best-mesh-refinement-option-in-the-FDTD-simulation-object

Yee cell with voxels having different media in its interior

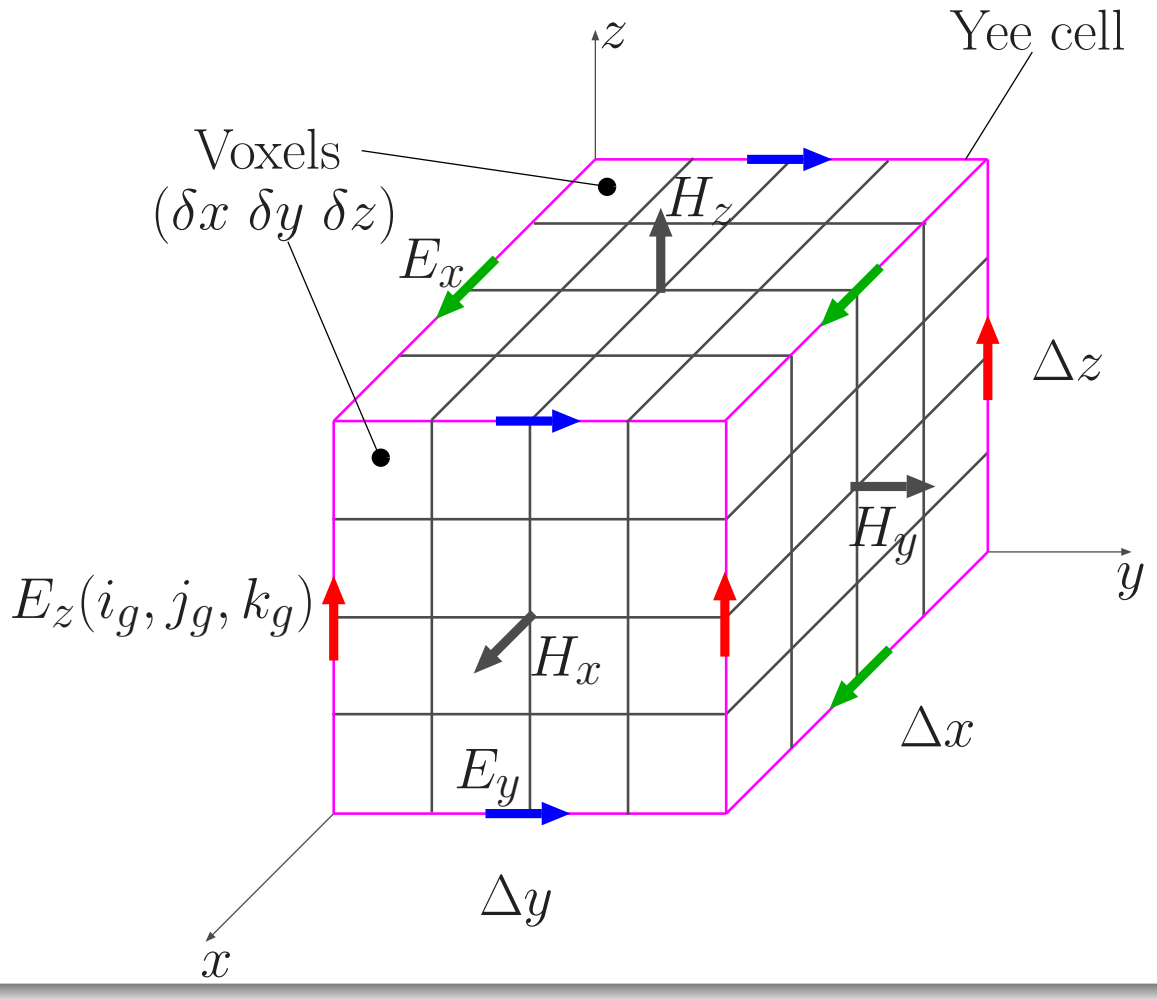

K. Tekbaş and J. Bérenger, "Finite-Difference Time-Domain (FDTD) Method with Non-Homogeneous Cells Filled with Voxels", in Journal of Computational Physics, vol. 489, pp. 112266, Jun. 2023, doi: 10.1016/j.jcp.2023.112266

E_z at the center

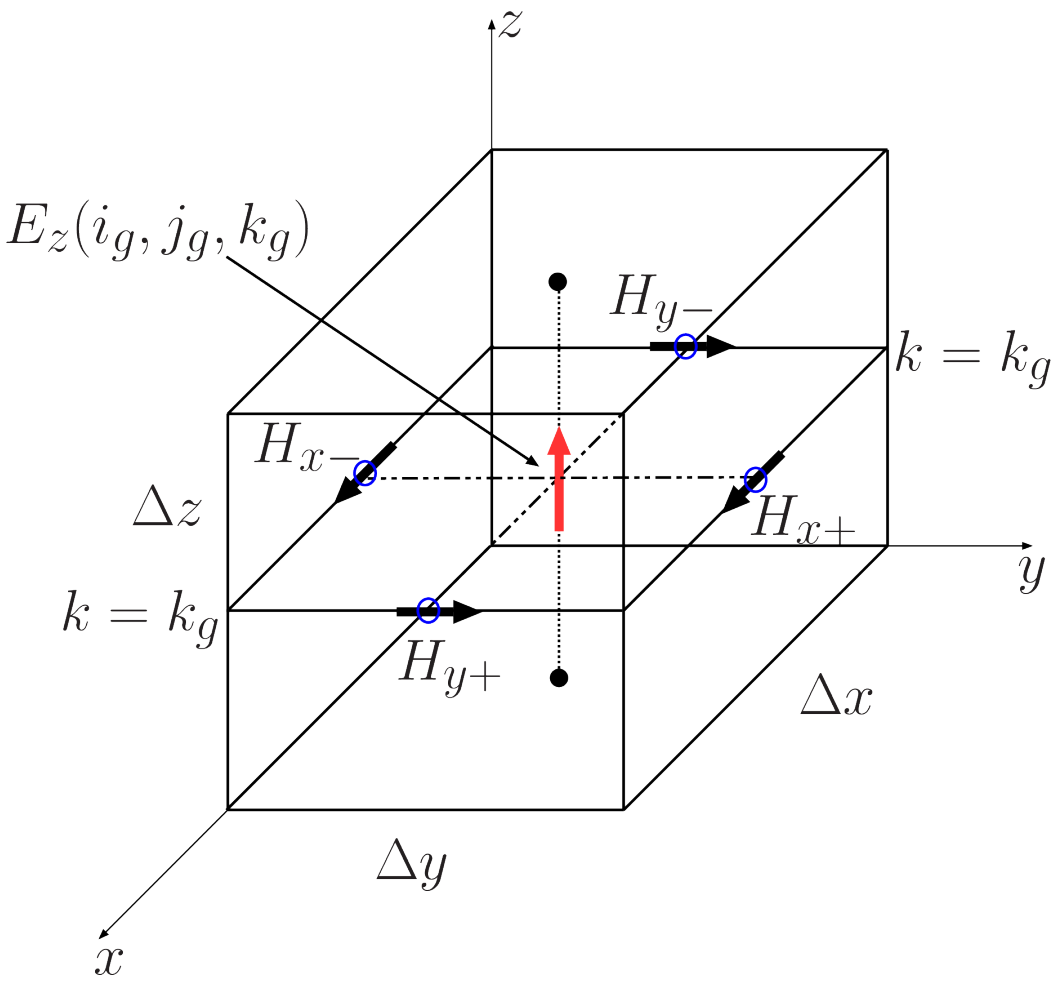

Discretizing the integral form of the Maxwell-Ampere equation

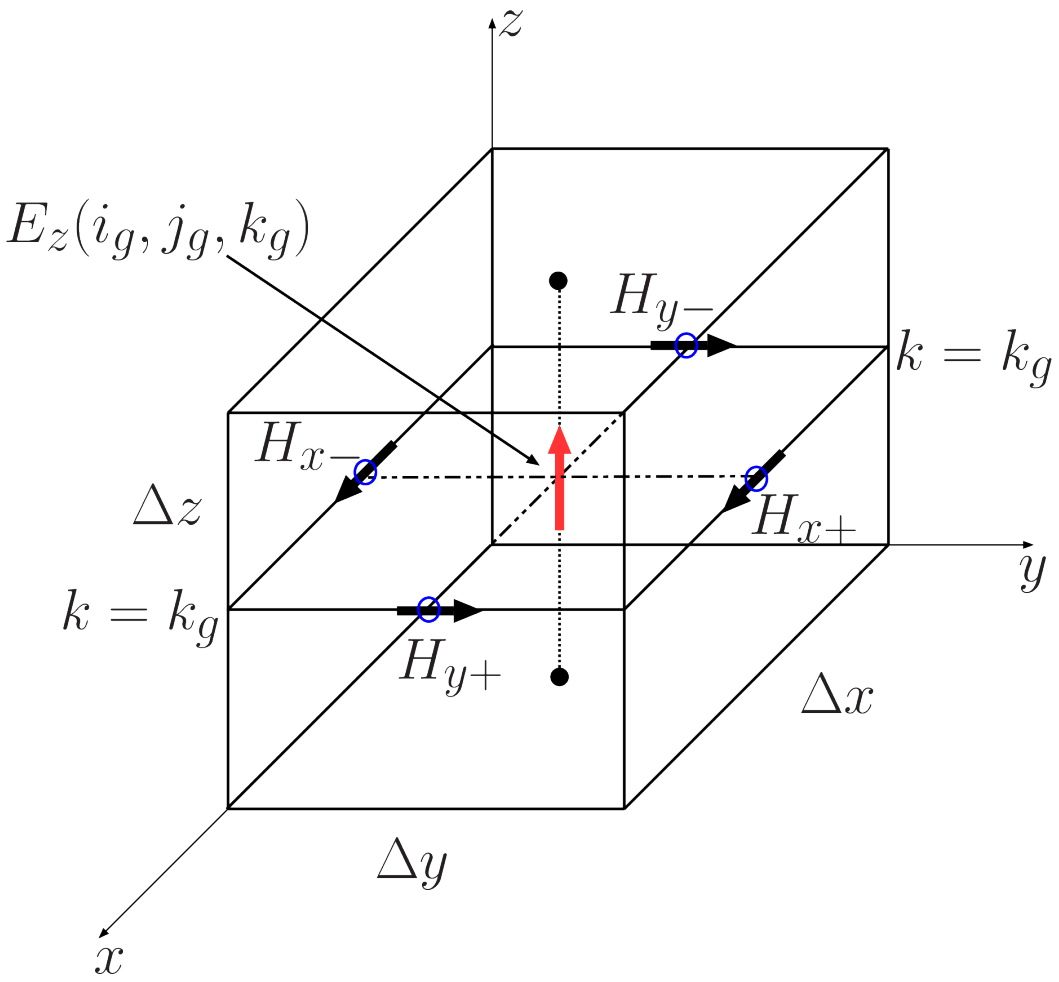

Maxwell-Ampere Law

$$\iint_{\Delta x \Delta y} \varepsilon \frac{\partial E_z(t)}{\partial t} dxdy = C_h(t)$$

$$C_h(t) = \int_L H(t) dl$$

$$E_z^{n+1}(i_g, j_g, k_g) = E_z^n(i_g, j_g, k_g) + \frac{\Delta t}{\varepsilon} \left[\frac{H_{y+}^{n+1/2} - H_{y-}^{n+1/2}}{\Delta x} - \frac{H_{x+}^{n+1/2} - H_{x-}^{n+1/2}}{\Delta y} \right]$$

Non-homogeneous cell composed with voxels

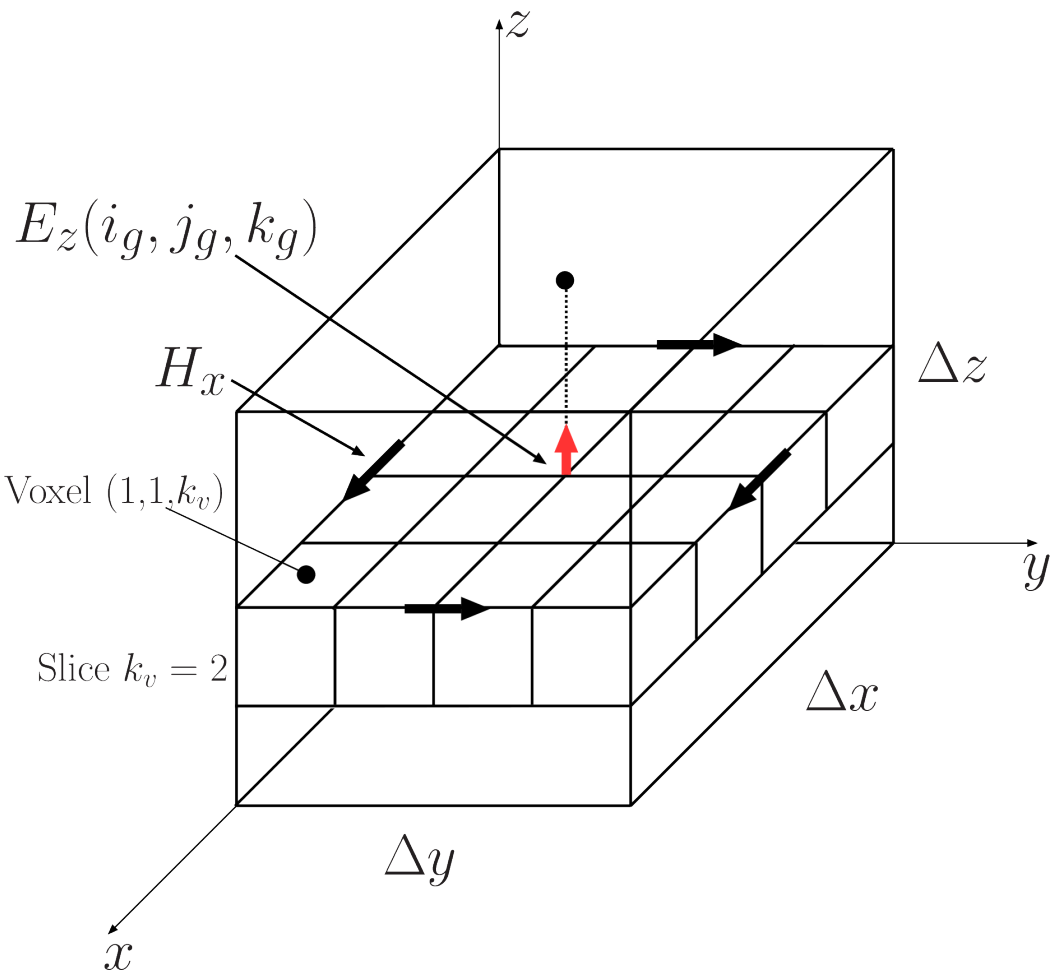

$$\sum_{i_v=1}^{M_i}\sum_{j_v=1}^{M_j}\varepsilon(i_v, j_v, k_v)\frac{\partial E_z(k_v, t)}{\partial t}\delta x\delta y = C_h(t)$$

$$\varepsilon^*(k_v) = \frac{\sum_{i_v=1}^{M_i}\sum_{j_v=1}^{M_j}\varepsilon(i_v, j_v, k_v)}{M_i M_j}$$

$$E_z^{n+1}(k_v) = E_z^n(k_v) + \frac{\Delta t}{\varepsilon^*(k_v)}\left[\frac{H_{y+}^{n+1/2} - H_{y-}^{n+1/2}}{\Delta x} - \frac{H_{x+}^{n+1/2} - H_{x-}^{n+1/2}}{\Delta y}\right] \quad (1)$$

Non-homogeneous cell composed with voxels

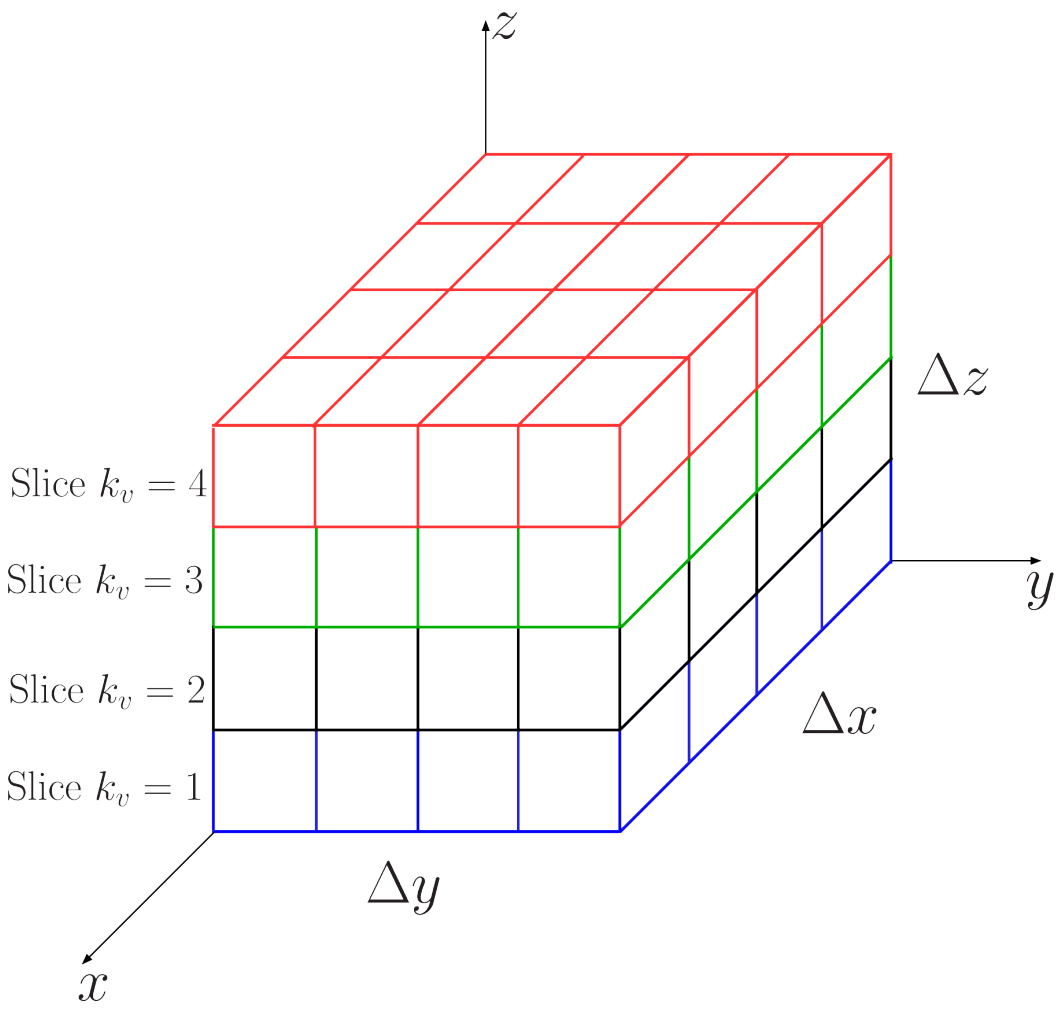

Maxwell-Faraday law in integral form,

In practice, since the integral is nothing but the average of over Δz, and since the permeability is homogeneous in the cells, the standard FDTD algorithm of the update of the H components can be left unchanged

$$E_z^{n+1}(i_g, j_g, k_g) = \frac{1}{M_k} \sum_{k_v=1}^{M_k} E_z^{n+1}(k_v) \tag{2}$$

The FDTD update of the E components

1. Compute $E_z^{n+1}(k_v)$ in each slice of the cell centered at $E_z^{n+1}(i_g, j_g, k_g)$ using (1),
2. Compute the average of $E_z^{n+1}(k_v)$ in the cell using (2), to be used later for the update of H components,
3. Proceed similarly for the E_x and E_y components.

Steps 1 and 2 can be merged and $E_z^{n+1}(i_g, j_g, k_g)$ computed as

$$E_z^{n+1}(i_g, j_g, k_g) = E_z^{n}(i_g, j_g, k_g) + \frac{\Delta t}{\varepsilon^{**}(i_g, j_g, k_g)} \left[\frac{H_{y+}^{n+1/2} - H_{y-}^{n+1/2}}{\Delta x} - \frac{H_{x+}^{n+1/2} - H_{x-}^{n+1/2}}{\Delta y} \right]$$

$$\frac{1}{\varepsilon^{**}(i_g, j_g, k_g)} = \frac{M_i M_j}{M_k} \sum_{k_v=1}^{M_k} \frac{1}{\sum_{i_v=1}^{M_i} \sum_{j_v=1}^{M_j} \varepsilon(i_v, j_v, k_v)}$$

The methods with which VIC is compared in the numerical experiments

1. Fine grid: the grid whose cell is superimposed to the voxels and has the same sizes $\delta x, \delta y, \delta z$
2. AVG: the coarse grid whose FDTD cell has same sizes $\Delta x, \Delta y, \Delta z$ and same location as the VIC cell

$$\varepsilon(i_g, j_g, k_g) = \frac{\sum_{i_v=1}^{M_i} \sum_{j_v=1}^{M_j} \sum_{k_v=1}^{M_k} \varepsilon(i_v, j_v, k_v)}{M_i M_j M_k}$$

The permittivity used to update E equals the average permittivity in the volume whose center is the considered E node.

- The difference between the VIC and AVG methods is like the difference between Luebbers and Maloney methods for thin sheets
- One takes account of the field discontinuity, the other does not.

2D VIC mesh with four voxels in each VIC cell ($\Delta x/\delta x = \Delta y/\delta y = 2$)

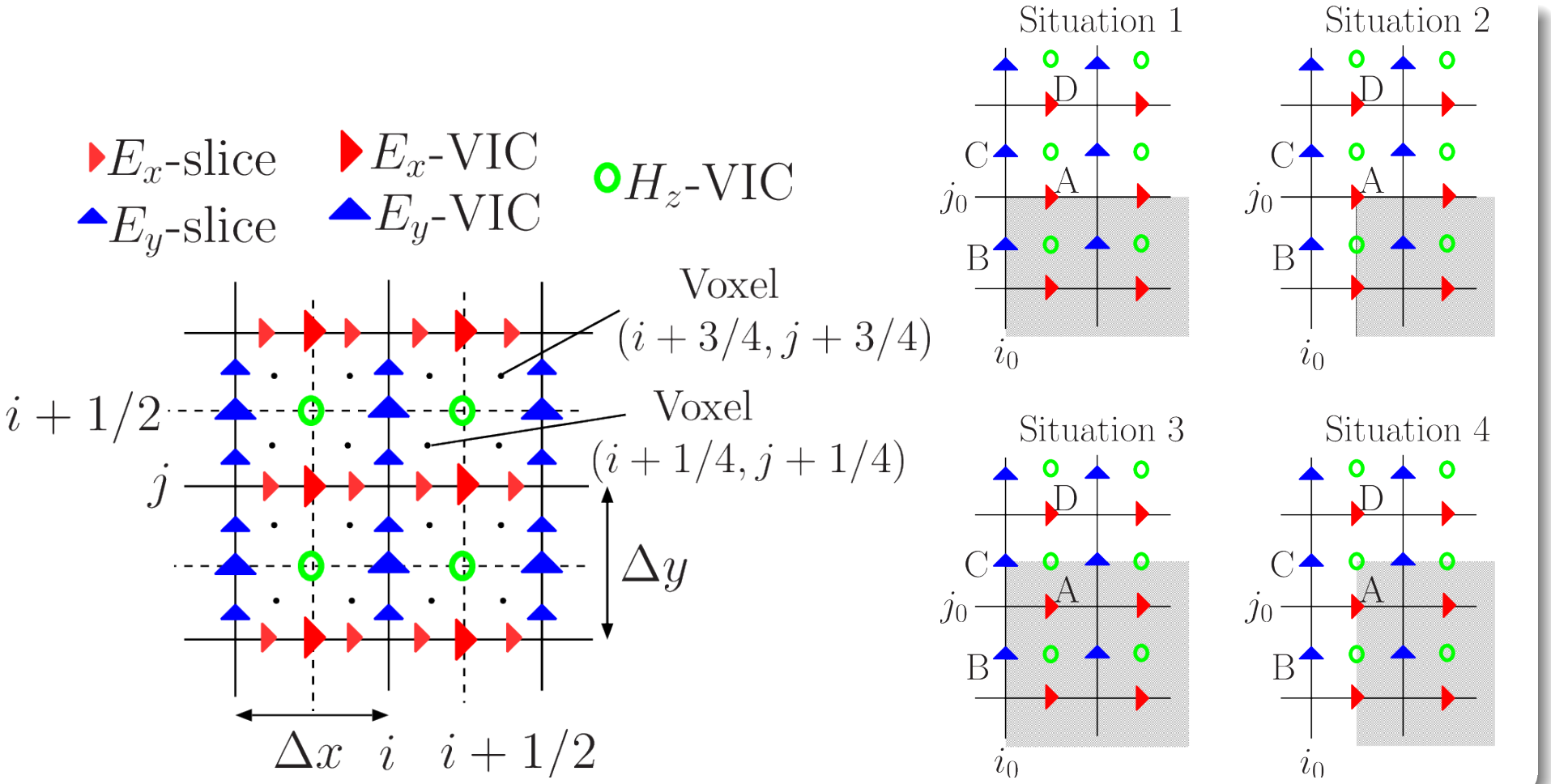

- The four situations of the corner of the square in the VIC grid
- **S1**: i_0, j_0 **S2**: $i_0 + 1/2, j_0$ **S3**: $i_0, j_0 + 1/2$ **S4**: $i_0 + 1/2, j_0 + 1/2$

Results at the corner with 20x20 square ($\varepsilon_r = 50$) in the VIC grid

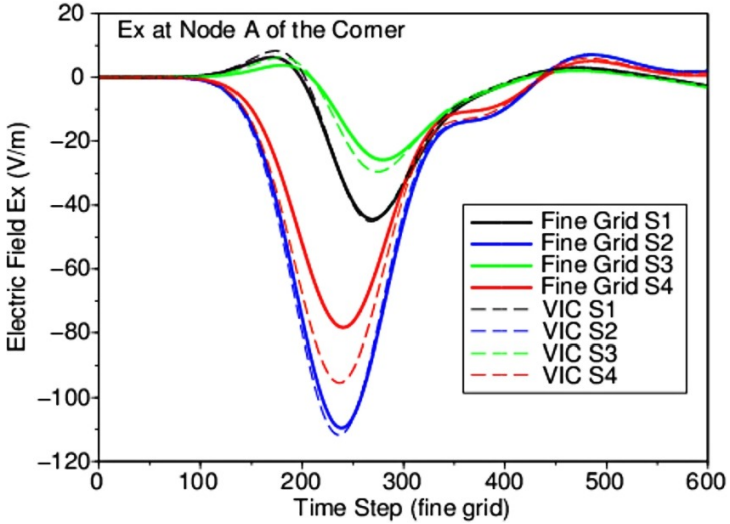

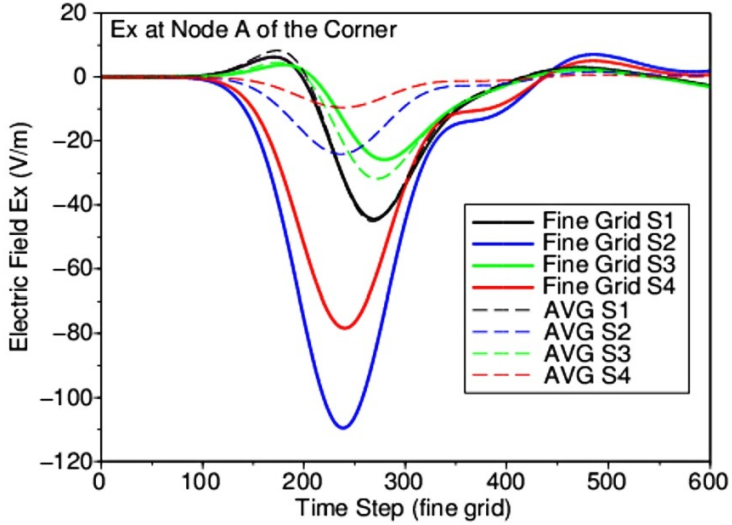

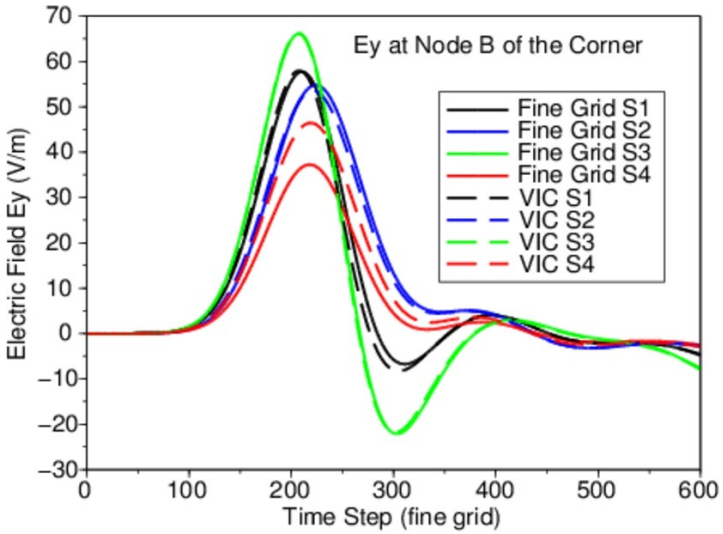

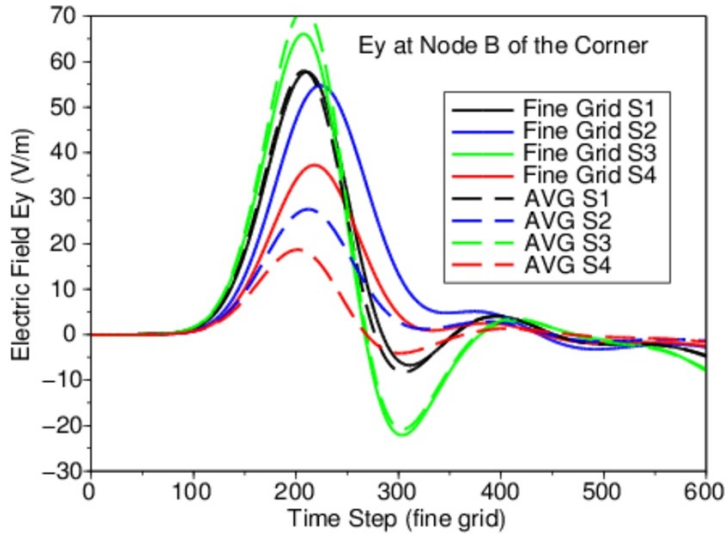

- The VIC results differ from the fine grid results with max. 10–15%.
- AVG is with a factor of the order of 4 or 5 in some cases.

E fields at nodes F, G, Q, and P

Outputted nodes:

- In the vicinity of the interface (nodes F and G)
- Far from the corner of the square (nodes Q and P)

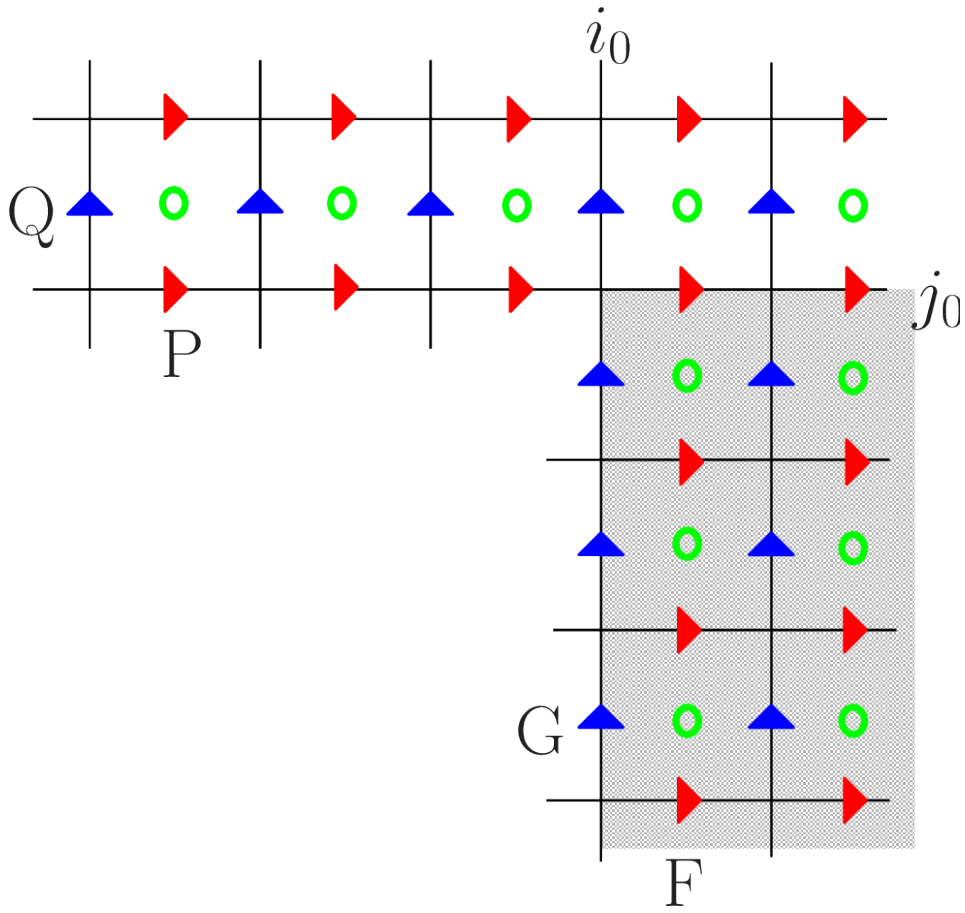

Results in the vicinity and far from the corner and the interface

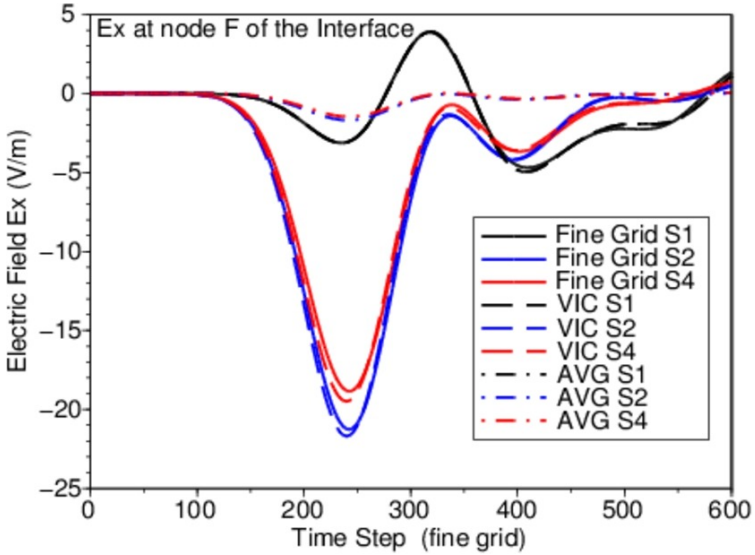

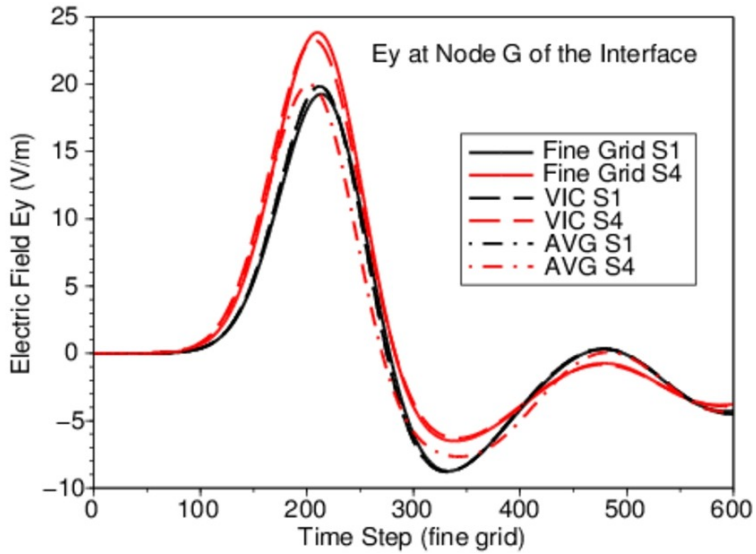

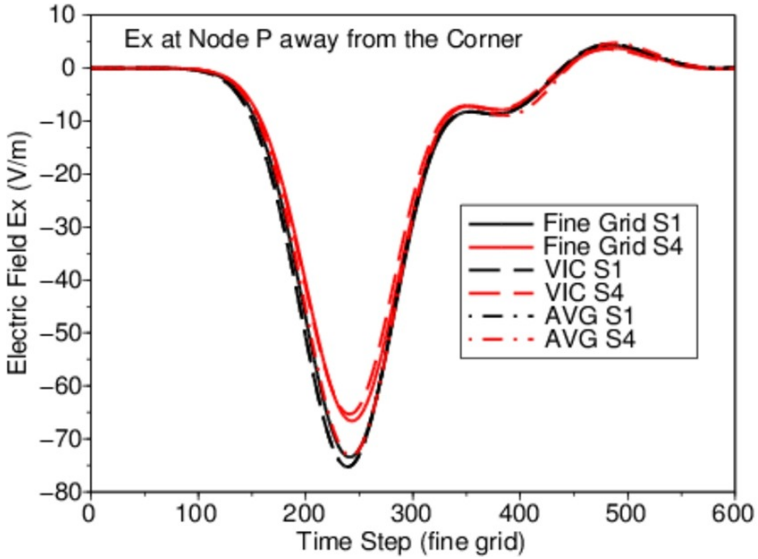

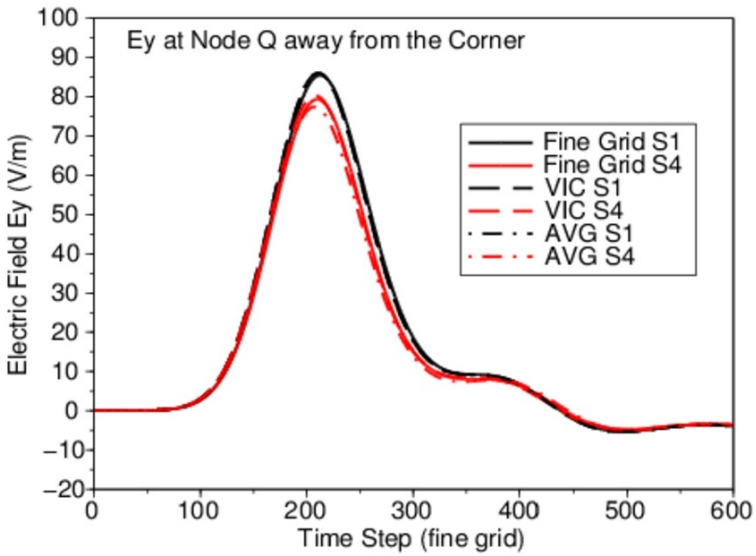

The corner in the VIC grid, 8 possible situations

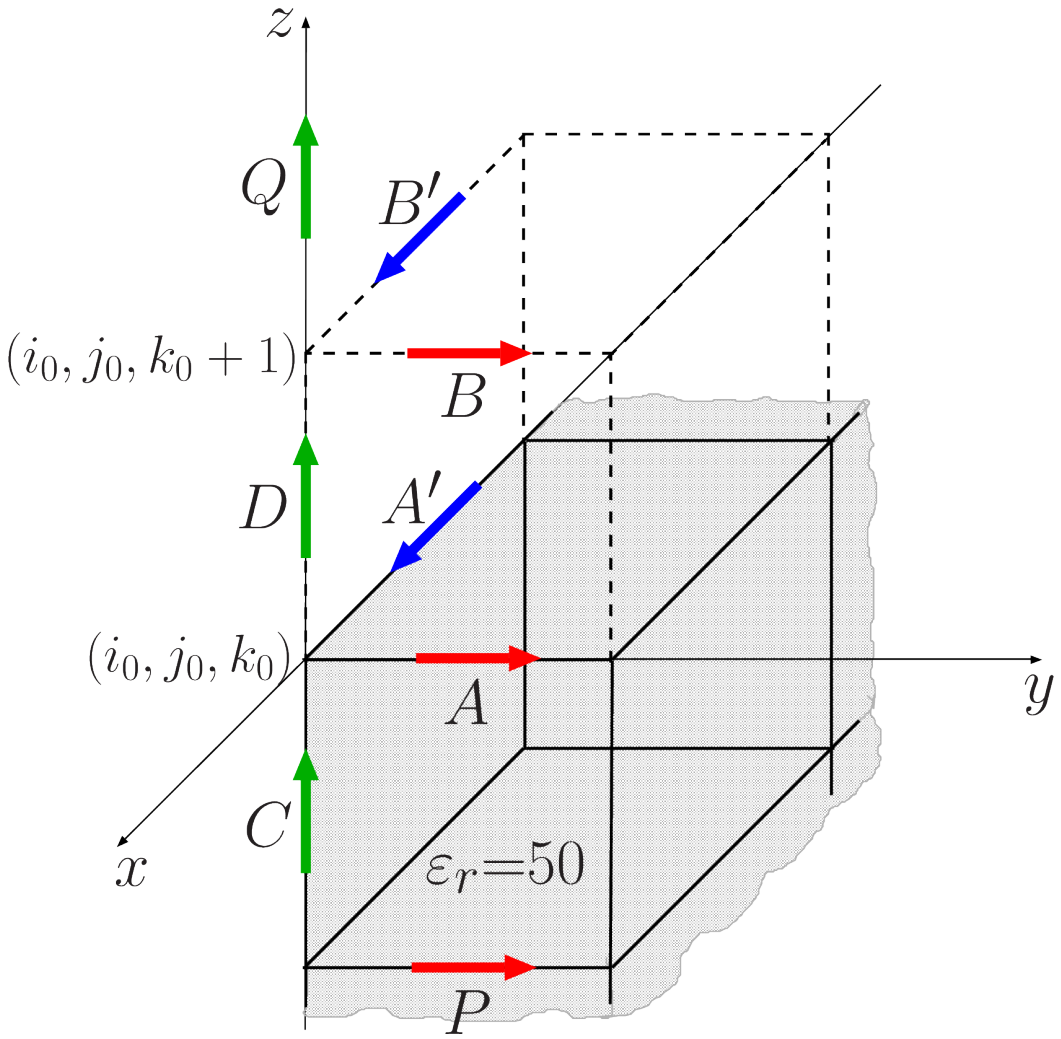

8 possible situations

- S1: i_0, j_0, k_0
- S2: $i_0 - 1/2, j_0, k_0$
- S3: $i_0, j_0 + 1/2, k_0$
- S4: $i_0 - 1/2, j_0 + 1/2, k_0$
- S5: $i_0, j_0, k_0 + 1/2$
- S6: $i_0 - 1/2, j_0, k_0 + 1/2$
- S7: $i_0, j_0 + 1/2, k_0 + 1/2$
- S8: $i_0 - 1/2, j_0 + 1/2, k_0 + 1/2$

The worst two and best two situations: Node A and Node C

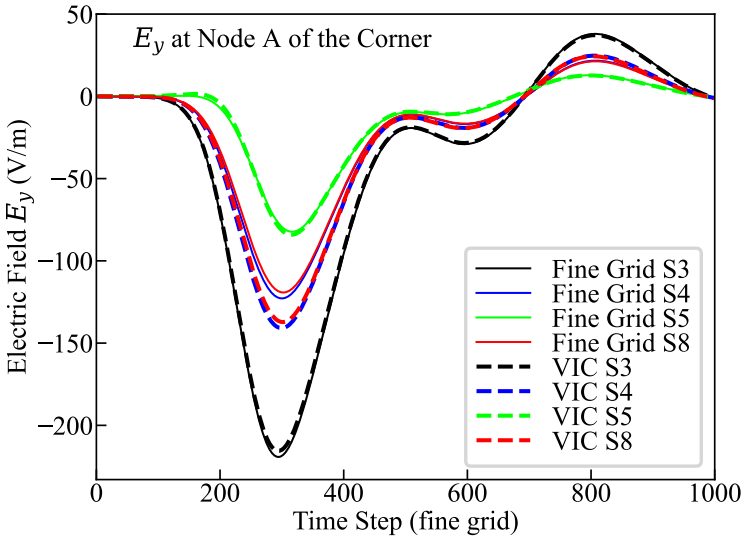

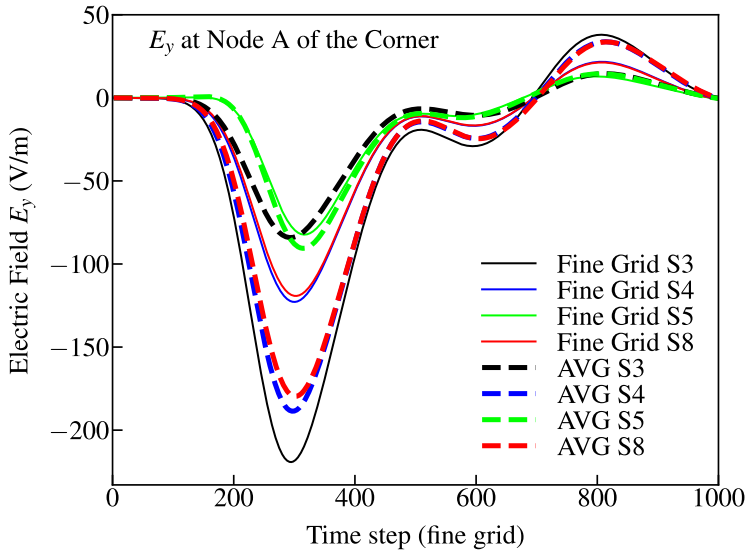

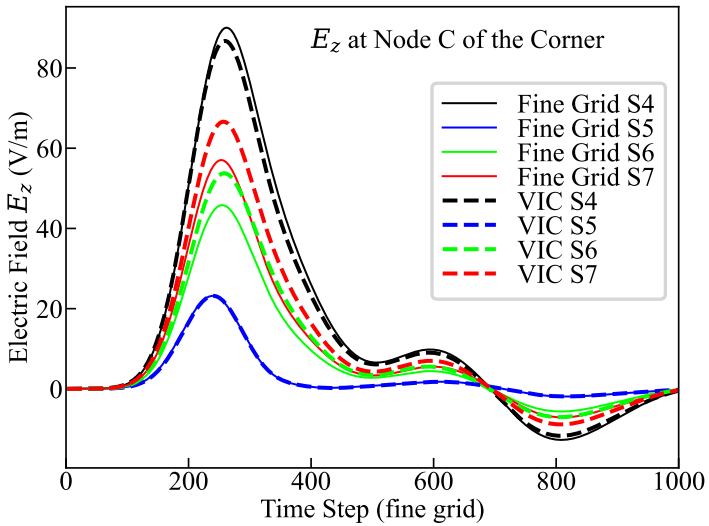

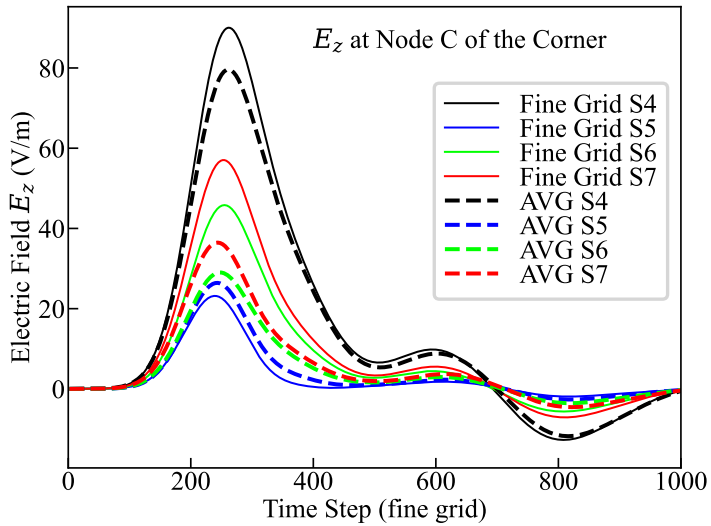

Experiments with an edge of a cube

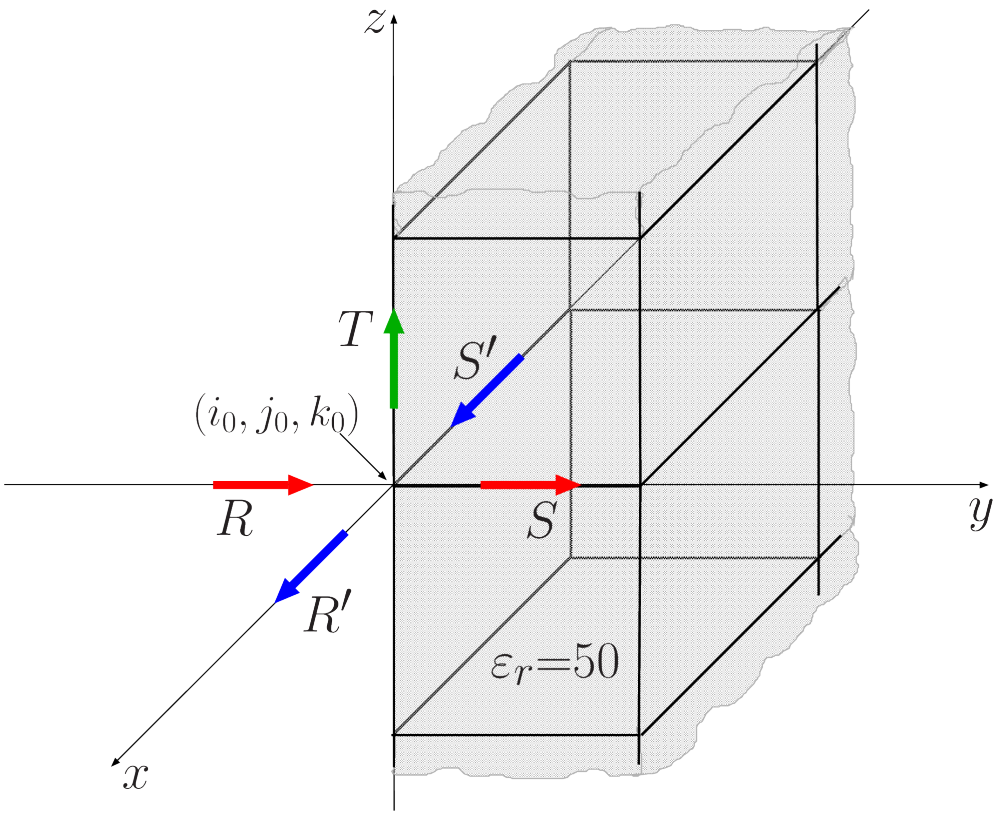

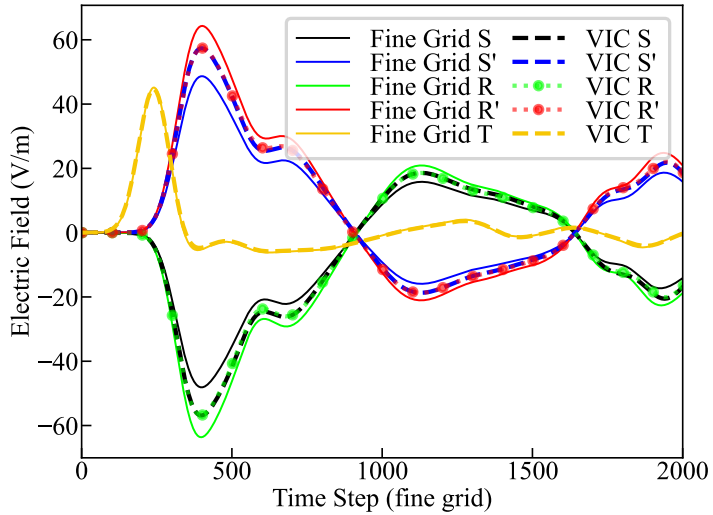

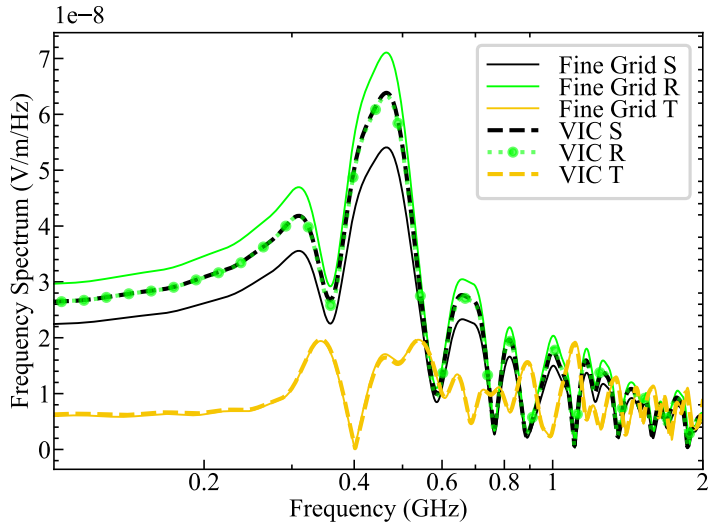

The *E* field parallel to the edge at T, which is not singular, is accurately computed

Remarks

- AVG can not account for the discontinuity of E normal to the interface
- The VIC method allows the computational burden to be reduced in comparison with fine mesh calculations ∴ the reductions of CPU times larger than one order of magnitude can be achieved
- The VIC method does not suffer from instability, the stability condition remains the CFL condition of the large VIC grid
- The upper bound of the frequency band is reduced by a factor of 2, which may be a limitation in some applications

Frequency dependency inclusion

The Debye media

- The one-pole Debye model

$$\epsilon_r(\omega) = \epsilon_\infty + \frac{\epsilon_S - \epsilon_\infty}{1 + \jmath\omega\tau} + \frac{\sigma}{\jmath\omega\epsilon_0}$$

ϵ_r	complex relative permittivity
ϵ_∞	optical relative permittivity
ϵ_S	static relative permittivity
ϵ_0	vacuum permittivity
ω	angular frequency
τ	characteristic relaxation time
σ	conductivity

- Broadband problems
- The most widely used $\cdot_{\cdot}\cdot$ simplicity of implementation
- Data fitting of the measurement data

Debye Media in the FDTD Method

- The relationship that connects the electric field and the electric flux density

$$D = \varepsilon_0 \left[\epsilon_\infty + \frac{\epsilon_S - \epsilon_\infty}{1 + \jmath\omega\tau} + \frac{\sigma}{\jmath\omega\epsilon_0} \right] E$$

- Making compatible with time domain using the auxiliary differential equation (ADE) approach

$$E_z^{n+1} = \alpha_1^{-1} \left[\alpha_2 E_z^n - \alpha_3 E_z^{n-1} + \Delta D_z^{n+1/2} - \beta \Delta D_z^{n-1/2} \right]$$

where

$$\alpha_1 = A + B + 0.5C, \qquad \alpha_2 = 2A + B - 0.5C, \qquad \alpha_3 = A, \qquad \beta = \tau/S$$

and

$$A = \varepsilon_0 \varepsilon_\infty \tau / S, \qquad B = (\varepsilon_0 \varepsilon_S + \sigma\tau)/S, \qquad C = \sigma(\Delta t)^2/S, \qquad S = \tau + \Delta t$$

FDTD Voxels-in-Cell method with Debye media

- The sole unknown $E_z^{n+1}(k_v)$ in each slice

$$E_z^{n+1}(k_v) = c_1(k_v)^{-1}\left[\frac{M_i M_j \Delta t}{\Delta x \Delta y} C_h^{n+1/2} + c_2(k_v) E_z^n(k_v) - c_3(k_v) E_z^{n-1}(k_v) - v(k_v)\right]$$

where

$$c_1(k_v) = \sum_{i_v=1}^{M_i}\sum_{j_v=1}^{M_j} \alpha_{1,i_v,j_v,k_v},\ c_2(k_v) = \sum_{i_v=1}^{M_i}\sum_{j_v=1}^{M_j} \alpha_{2,i_v,j_v,k_v},\ c_3(k_v) = \sum_{i_v=1}^{M_i}\sum_{j_v=1}^{M_j} \alpha_{3,i_v,j_v,k_v}$$

$$v(k_v) = \sum_{i_v=1}^{M_i}\sum_{j_v=1}^{M_j}\left[\beta_{i_v,j_v,k_v} \Delta D_z^{n-1/2}(i_v, j_v, k_v)\right]$$

- The value of $E_z^{n+1}(i_g, j_g, k_g)$ field at the center of cell

$$E_z^{n+1}(i_g, j_g, k_g) = \frac{1}{M_k}\sum_{k_v=1}^{M_k} E_z^{n+1}(k_v)$$

K. Tekbaş, J. Bérenger, L.M. Angulo, MR Cabello and S. Garcia "FDTD Voxels-in-Cell method with Debye media", submitted to IEEE Trans. on Antennas and Propag., vol. 72, no. 5, pp. 4431-4439, May 2024.

Voxel-Based Human Head Model

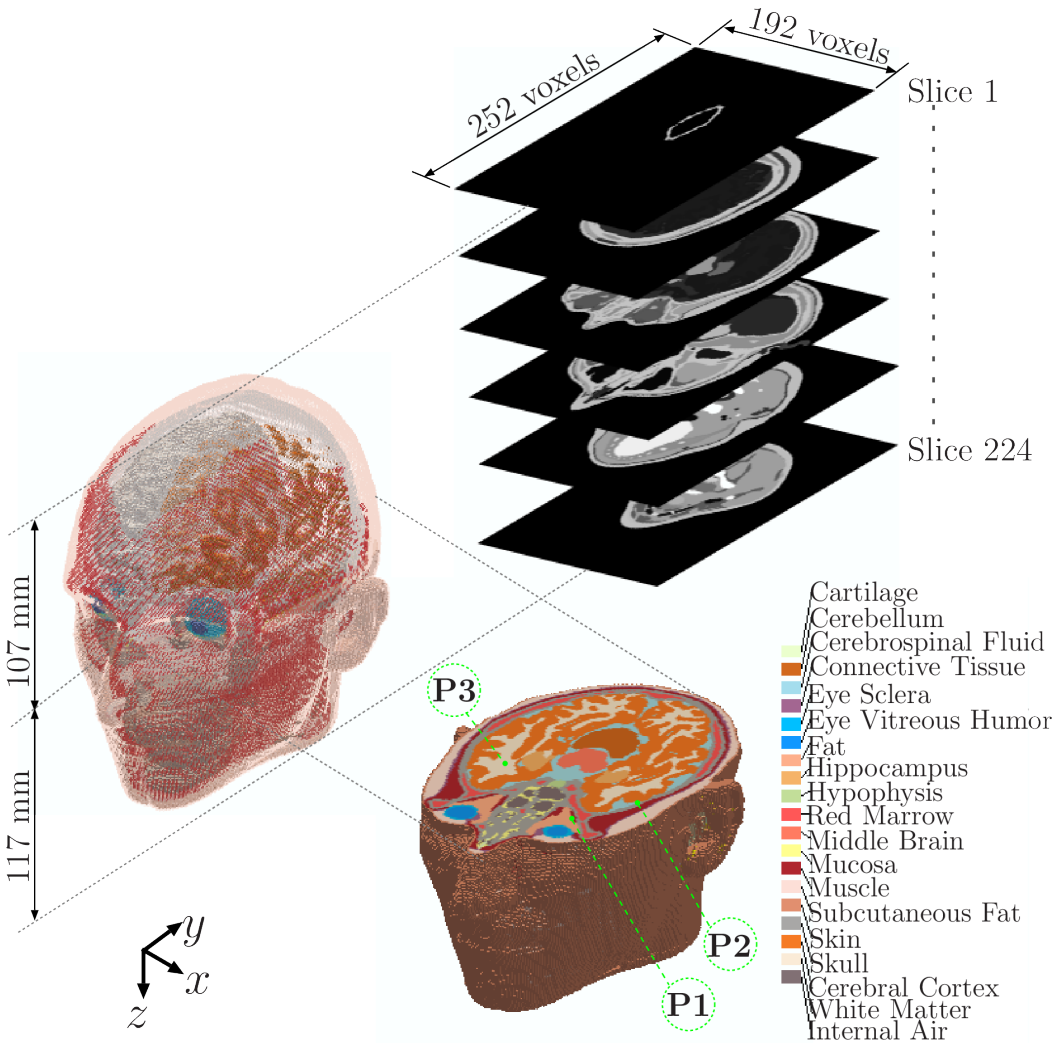

	σ (S/m)	ϵ_S	ϵ_∞	τ (ps)
Cartilage	0.494	44.5	19.4	18.8
Cerebellum	0.826	58.2	35.2	68.3
Cerebrospinal Fluid	2.144	70.4	33.1	18.2
Connective Tissue	0.540	46.7	16.7	12.9
Eye Sclera	0.924	56.5	28.2	12.8
Eye Vitreous Humor	1.445	67.7	10.3	82.7
Fat	0.037	5.53	4.00	23.6
Hippocampus	0.595	56.4	33.1	35.2
Hypophysis	0.809	60.5	27.7	17.7
Red Marrow	0.104	14.2	7.36	34.1
Middle Brain	0.826	58.2	35.2	68.3
Muscle	0.747	56.93	28.00	18.67
Subcutaneous Fat	0.037	5.53	4.00	23.6
Skin	0.540	47.9	29.9	43.6
Skull	0.104	14.2	7.36	34.1
Cerebral Cortex	0.595	56.4	33.1	35.2
White Matter	0.348	41.3	24.4	33.6
Internal Air	0.000	1.00	1.00	0.00

A. Christ et al., "The virtual family—Development of surface-based anatomical models of two adults and two children for dosimetry simulations", Phys. Med. Biol., vol. 55, no. 2, pp. N23-N38

Results in Eye Ball, Skull, White Matter and Average Error

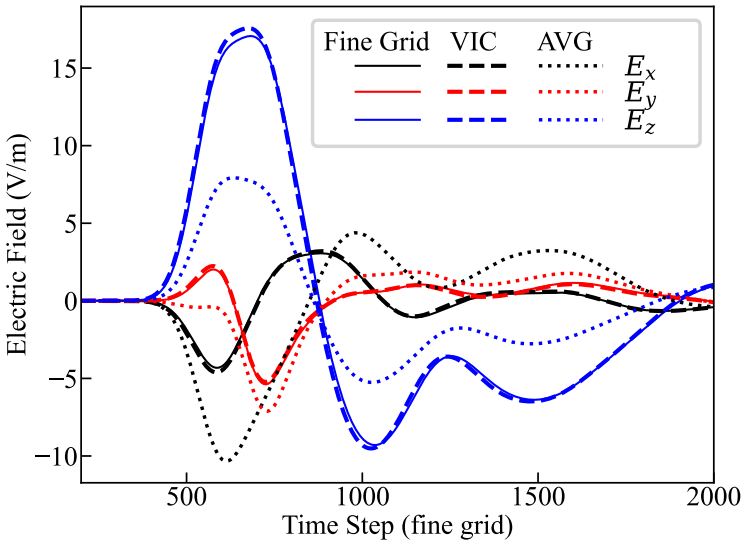

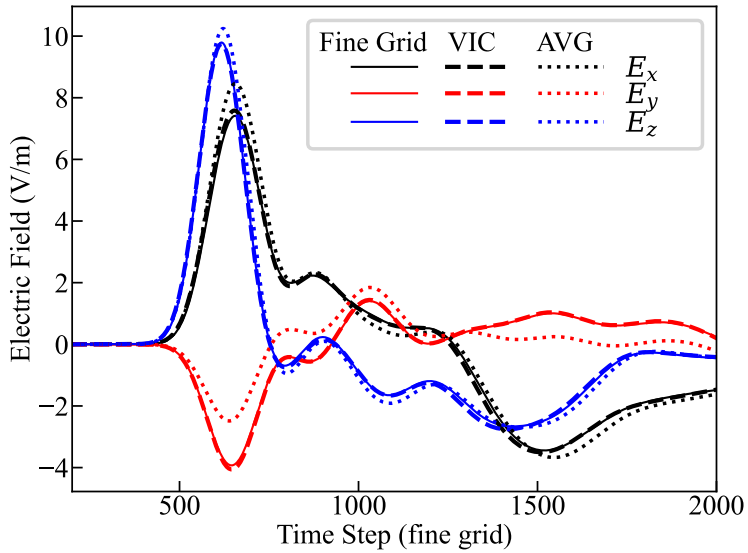

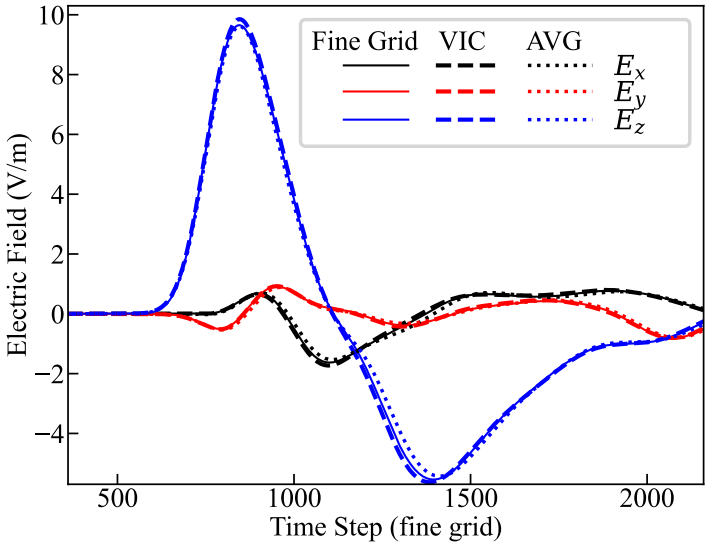

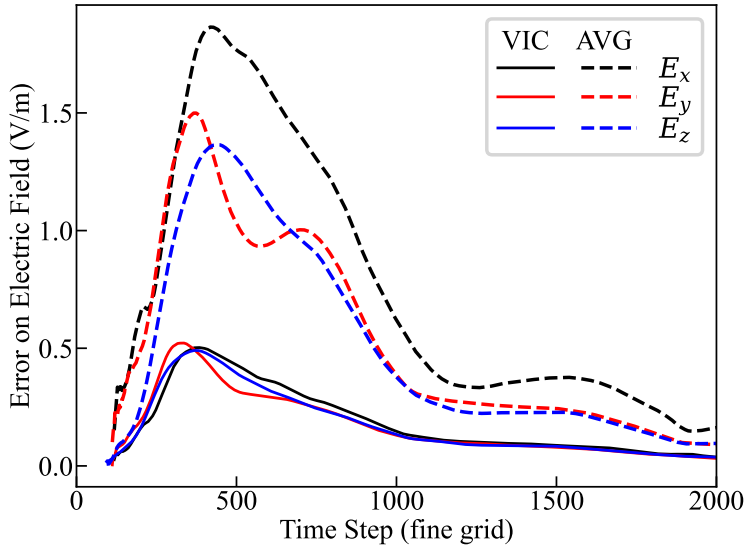

The pure dielectric case vs Debye case

The presence of loss terms with the Debye media

- The magnitude of the field, especially its peak value, is lower with the Debye media than with the pure dielectric media.
- The oscillations of the field are significantly reduced

Both differences were expected, because of loss terms with the Debye media, while the pure dielectric media are lossless.

The complex constitutive relation of the Debye media

- The reduction of the computational requirements is lesser than with dielectric objects

But it remains high compared to fine mesh case, especially for the CPU time which is reduced by about one order of magnitude with VIC cells two times the voxels size.

Further details about the VIC method can be found in the references below

1. Tekbas, K. and Berenger, J.-P., "Finite-Difference Time-Domain (FDTD) Method with Non-Homogeneous Cells Filled with Voxels", Journal of Computational Physics, vol. 489, pp. 112266, Sep. 2023, https://doi.org/10.1016/j.jcp.2023.112266

2. Tekbas, K., Berenger, J.-P., Angulo, L. D., Cabello, M. R., and Garcia S., "FDTD Voxels-in-Cell method with Debye media", IEEE Transactions on Antennas and Propagation, vol. 72, no. 5, pp. 4431-4439, May 2024, https://doi.org/10.1109/TAP.2024.3378847

3. Tekbas, K., Berenger, J.-P., Angulo, L. D., Cabello, M. R., and Garcia S., "Accelerating Finite-Difference Time-Domain (FDTD) Solvers using Voxels-in-Cell Method", 2024 IEEE International Symposium on Antennas and Propagation and INC/USNC-URSI Radio Science Meeting (AP-S/INC-USNC-URSI), Firenze, Italy, 2024, pp. 213-214, https://doi.org/10.1109/AP-S/INC-USNC-URSI52054.2024.10687154